

Electrofacies and Depositional Environment Analysis of the Paleogene-Neogene in Tainan Basin

CHING-CHIUAN SU¹, CHIA-SHENG TU¹, ANDREW TIEN-SHUN LIN², and PING-JUNG HSIEH¹

ABSTRACT

Electrofacies are widely used for interpreting depositional environments based on well log patterns, although there are still some uncertainties. To improve the accuracy of the lithology interpretation, this study integrated the lithology description from subsurface geology well report with well log patterns to define the electrofacies. The F-8 well was taken as the standard electrofacies column for analyzing the depositional environment and understanding its evolution. Furthermore, we divide the Paleogene-Neogene strata into 8 depositional environments including slope, turbidite, outer offshore, inner offshore, shoreface, outer coast, inner coast, and non-marine. Based on the changing trend in depositional environments, the Oligocene-Pliocene strata are divided into 17 sequences for regional correlation in the Tainan Basin. We created some correlation profiles of sequence strata in the Tainan Basin and integrated them with the eustatic curve, tectonic activities to explain the geological framework from Oligocene to Pliocene. The sequence set A, deposited in the period from the late Oligocene to early Miocene, experienced the early post-breakup activities. The sequence set B and C, deposited in the period from the early Miocene to middle Miocene, experienced the relatively quiet period of tectonic activities with added accommodation mostly from thermal subsidence. The sequence set D, deposited in the period from the middle Miocene to late Miocene, experienced some renewed extension activities. The subsidence area formed by the renewed extension activities was called the Northern Depression. The rapidly increasing accommodation was inconsistent with the trend of the eustatic sea-level curve due to the extensional subsidence. The Central Uplift

Zone and the south of the Northern Depression commonly lack sequence set D. It is inferred that there should be a fault between the F-6 and F-8 wells acting as a tectonic boundary. The Pliocene strata were generally missing in the period from NN12 to NN14, corresponding TB3.5 cycle. We infer that the hiatus could result from forebulge deformation. The thick Pliocene strata should be formed under the development of the foredeep basin.

Key words: electrofacies, sequence stratigraphy, Tainan Basin

CHING-CHIUAN SU: 155764@cpc.com.tw

¹ Exploration and Development Research Institute, CPC Corporation, Taiwan

² Department of Earth Sciences, National Central University, Taiwan

GENERAL GEOLOGY OF THE STUDY AREA

During the Cretaceous, the Taiwan Strait was on the passive margin of the eastern Eurasian continental plate. After the Paleocene, the crust began to breakup and rift forming a series of north-east normal faults, forming multiple rifted basins. The strata of these rifted basins were composed of Cenozoic sedimentary rocks. It records the tectonic evolution process between rift-drift, thermal subsidence, and foreland loading during the Cenozoic of the Taiwan Strait (Teng, 1987; Teng, 1990; Teng and Lin, 2004).

According to the stratigraphic analysis of seismic reflection data, it is known that the rifted basins experienced two episodes of tectonic events (Lin et al., 2002; 2003). The first episode was the continent breakup stage: The eastern margin of the Eurasian Plate is a subduction zone until Cretaceous and turned into a passive margin from Paleocene to Early Oligocene (~58-30Ma). Until the late Eocene (~37Ma), the crust began to breakup and rift forming a series of north-east normal faults, resulting in multiple half-grabens and horsts. Due to local unconformities caused by the uplifting of the horst or falling of sea-level, these half-graben turn into Nanjihtao Basin, Taihsi Basin, Penghu Basin, and Tainan Basin from north to south (Fig. 1).

The second episode was the post-breakup stage: from the late Oligocene to the late Miocene (30-6.5 million years ago). The behavior of normal faults had slowed down and turned into regional thermal subsidence. The accommodation caused by rapid subsidence made the sediment overly the horsts. Therefore, the Miocene strata were widely distributed and conformable (Sun, 1985; Lin et al., 2003). The sources of sediment supply mainly came from the South China Continental in the west and the exposed horst during sea-level falling in Taiwan Strait. After comparing the depositional environment of the Western Foothill strata between north and south, it can be inferred that the water depth of the basin was deeper to the south.

About 15 million years ago, the northern Luzon volcanic arc began moving toward the Eurasian continental plate northwestward. After the Late Miocene, the volcanic arc collided with the Eurasian Plate, causing orogenic activities

(Teng, 1990). The loading of the orogen caused western Taiwan to sink, forming a foreland basin. At this time, the denudation of the uplifted mountains supplied a large amount of sediment to the foreland basin. The seismic reflection and well data of the offshore area revealed that there is a Basal Foreland Unconformity (BFU). As the form of stratigraphic stacking above the BFU is very different from the underlying strata, it is inferred that the timing of the development of the foreland basin was about 6.5 million years ago (Lin et al., 2002; 2003).

The Tainan Basin, a northeast-southwest trend half-graben basin, was the southernmost rift basin in the Taiwan Strait (Sun, 1985). The tensional depression resulted in a series of normal faults with a northeast-southwest trend. Based on the distribution of major normal faults, the Tainan Basin can be divided into three zones: Northern Depression, Central Uplift Zone, and Southern Depression (Lee et al., 1995), as shown in the red box in Fig. 1.

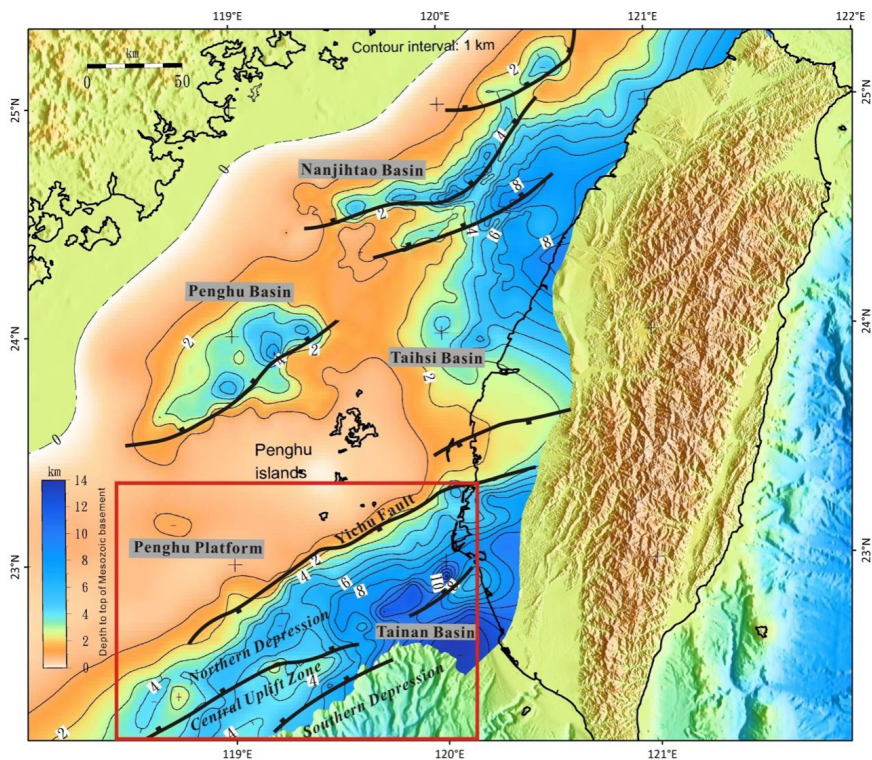


Fig. 1. The regional geology map of the Taiwan Strait is modified from Lin (2003). The contour lines of the Cenozoic sediment isopach are shown in km. Thick black lines on this isopach map are major normal faults. The red box indicates the Tainan Basin.

PROCEDURES

Most of the drilling data in the Tainan Basin were from the central uplift. The wells in Northern Depression are relatively scattered, while in Southern Depression are absent. To understand the depositional environment and tectonic evolution of the Tainan Basin, we have to establish sequence stratigraphy correlation profiles. Therefore, we choose 9 wells, including C-1, P-1, Y-1, J-1, FF-1, F-8, F-6, F-10, and M-1, from Northern Depression and Central Uplift Zone for better correlation (the green line in Fig. 2).

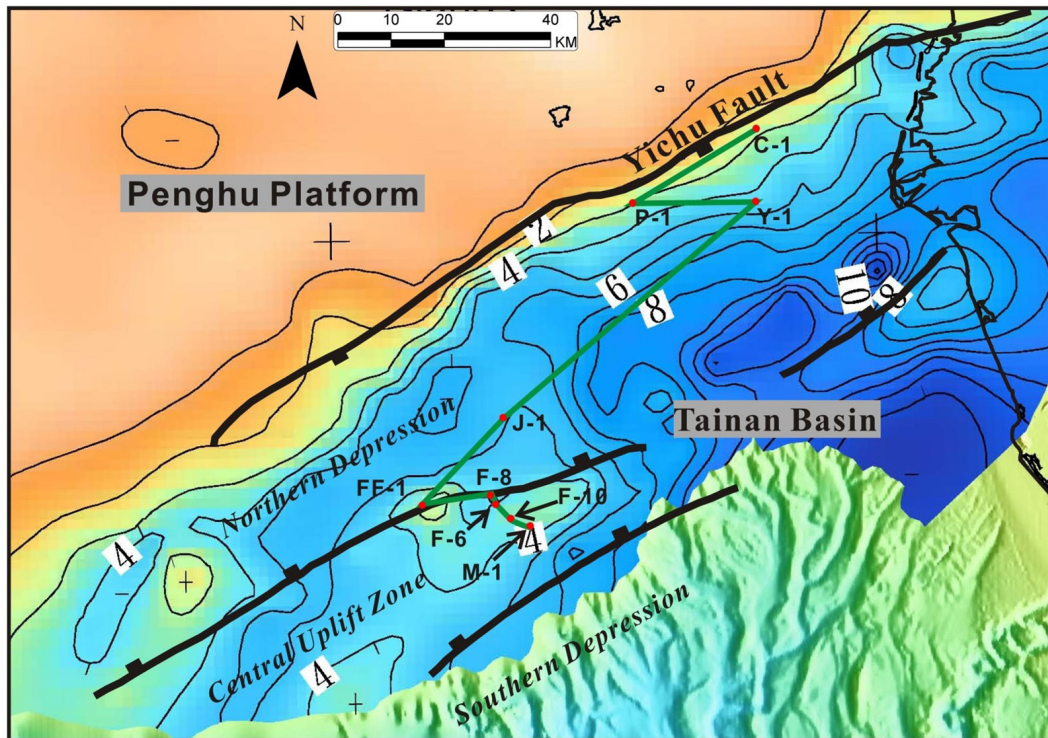


Fig. 2. The regional geology map of the Tainan Basin is modified from Lin (2003). Borehole data are shown as red circles, and connected by the green line as sequence stratigraphy profile in this study.

By integrating the previously identified nannofossil zones (Table 1) with the logging, core, and cutting descriptions, we could speculate the depositional environment, and sequence stratigraphy of the Tainan Basin.

To have a complete chronostratigraphic and depositional environment analysis standard, we use the F-8 well, located at the northern margin of the F structure with fewer hiatus, as the standard well for analyzing the depositional environment. The analysis steps are as follows: 1. Lithology column to be built; 2. Electrofacies and depositional environment analysis; 3. Sequence stratigraphic analysis.

Table 1. The nannofossil zones of the 9 wells used in this study (compiled from subsurface geological reports).

Age	Nanno zone Top	Unconformity	C-1	P-1	J-1	Y-1	FF-1	F-8	F-6	F-10	M-1	
Pleistocene	NN19-21		143	76.32	98.82	142.5	88.5	187	110	128	141	
Pliocene	Late	NN17-NN18	550	7390	1320	900	1730	1160	1190	1170	1400	
		NN16	600		1736	1388	1778	///////		1690	1536	
	Early	NN15	630	550	2084	1550	///////	///////	1850	1750	1648	
		NN14					///////	///////	///////	///////	2082	
		NN13		///////	///////	///////	///////	///////	///////	///////	///////	
		NN12		///////	///////	///////	///////	///////	///////	///////	///////	
Miocene	Late		S.U.5		2325		1845	1827	1904	1775	2390	
		NN11		910	1140	2378	2103	1855	1850	1910	1800	2425
		NN10				2761	2535	///////		///////	///////	///////
	Middle	NN9		1967	1721	3025	2600	///////	2502	///////	///////	///////
		NN8			2000	3252		///////	2627	///////	///////	///////
		NN7					3038	///////	2693	///////	///////	///////
			S.U.4		2300			2186			1805	2474
		NN6		2160		3653	3165	2217	2792		#####	///////
		NN5		2267	2600	3736	3388	2220	2822	1980	1825	///////
	Early	NN4		2450	2710	3980	3505	2490	3000	2015	1960	///////
		NN3			2820	4261	3775	2587	3125	2243	2140	#####
		NN2				///////	4050	2854	3320	2305	2755	2528
NN1			///////	///////	///////							
		S.U.3							3610		3120	
Oligocene	Late	CN1a		///////	///////	///////	///////	///////	3725	3460	#####	
			S.U.2								3163	
		NP25		///////	///////	///////	///////	///////	3843	3700	#####	3127.5
		NP24		///////	///////	///////	///////	///////	3952	3850	3234	3144
			S.U.1		2564	2889	4764	4300	2980	4039	4022	3341
Cretaceous			2564	2889	4764	4300	2980	4039	4022	3341	3155	
Jurassic										3724	3296	
Total depth(meter)			2907	3437	4862	4327	3350	4110	4100	3805	3557	
Remark	///// : Hiatus ##### : Partly Missing											

Based on our depositional environment analysis and the geological framework established previously, the sequence boundaries of each well can be correlated in the stratigraphic profile. It helps create the stratigraphic framework of the Tainan Basin, which might reveal the relationship between sequence strata, eustatic curve, and tectonic event in the Tainan Basin.

BUILD LITHOLOGY COLUMN

The lithology in the composite log is the fundamental data by observation of cuttings. The descriptions of lithology include texture, composition, and sediment contents. However, the depth of the cuttings still needs to be corrected by well log data. The accuracy of the lithology interpretation can be improved by integrating the analysis results of rock description with well log data.

The lithology column was built based on the rock description from the composite log in the well geological report. The lithology was classified into seven groups: Shale, Silty Shale, Carbonaceous Shale, Muddy Sand, Sand, Limestone, and Coal. Fig. 3 shows the procedure of building the lithology column. The example column is from 3,500 to 3,600 meters in depth. The lithology description of rock is visualized and digitalized in the lithology column.

Well logs are commonly used for regional stratigraphic correlation. This study uses the 1:2000 scale Gamma Ray (GR), resistivity, and density log chart as the basis for both electrofacies and depositional environment analysis. Geologists usually use the GR Log to determine the shale content of sediments. Generally, a high GR value indicates high shale content, and a low GR value indicates sandstone with low shale content. This study integrates the lithology column with GR trends. The visualization shows the trend of lithology changes with depth. This can be used to understand the trends of particle size and the stacking pattern (such as fining upward or coarsening upward), as shown in Fig. 4.

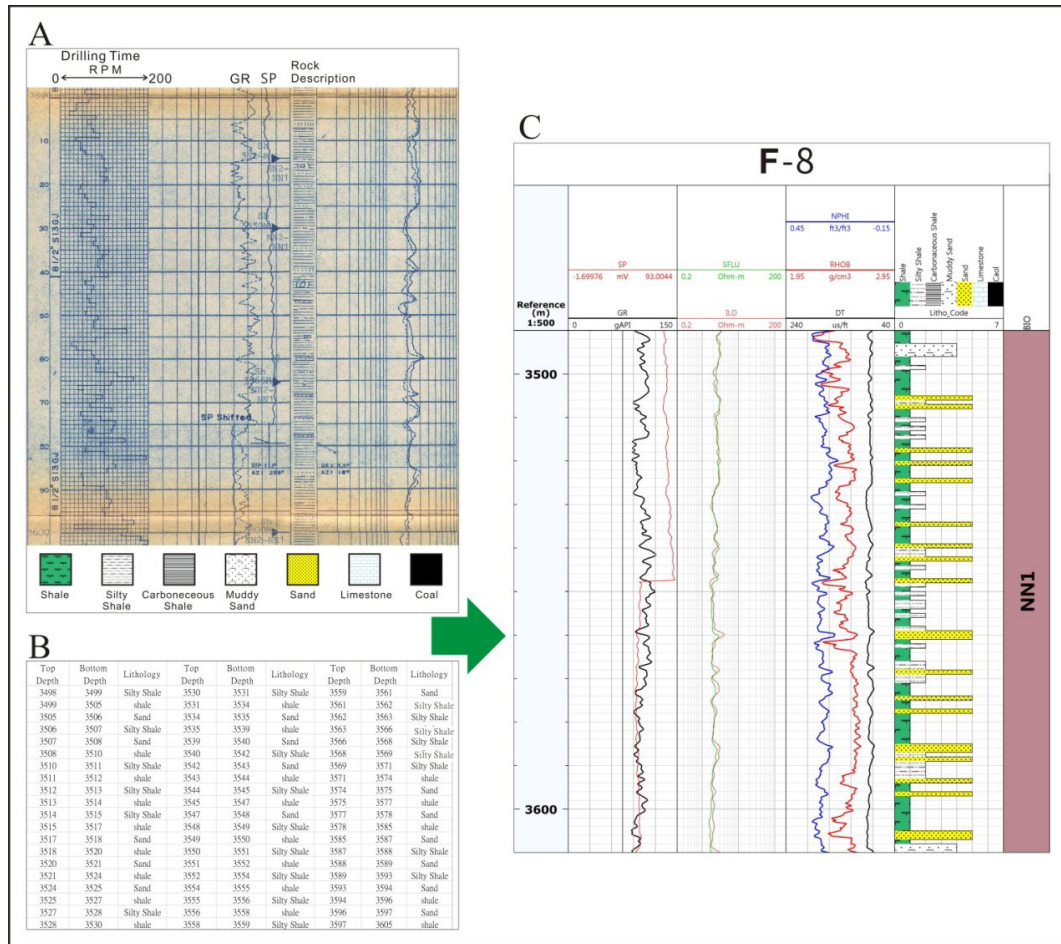


Fig. 3. The process of creating a lithology column. The F-8 well is used as an example. Figure A shows the composite log in subsurface geological report of the well F-8, the section is around 3,500-3,600 m at depth. In figure B, we demonstrate the zonation of lithology based on the composite log. In figure C, we create the lithology column by integrating the log data with the interpreted lithology.

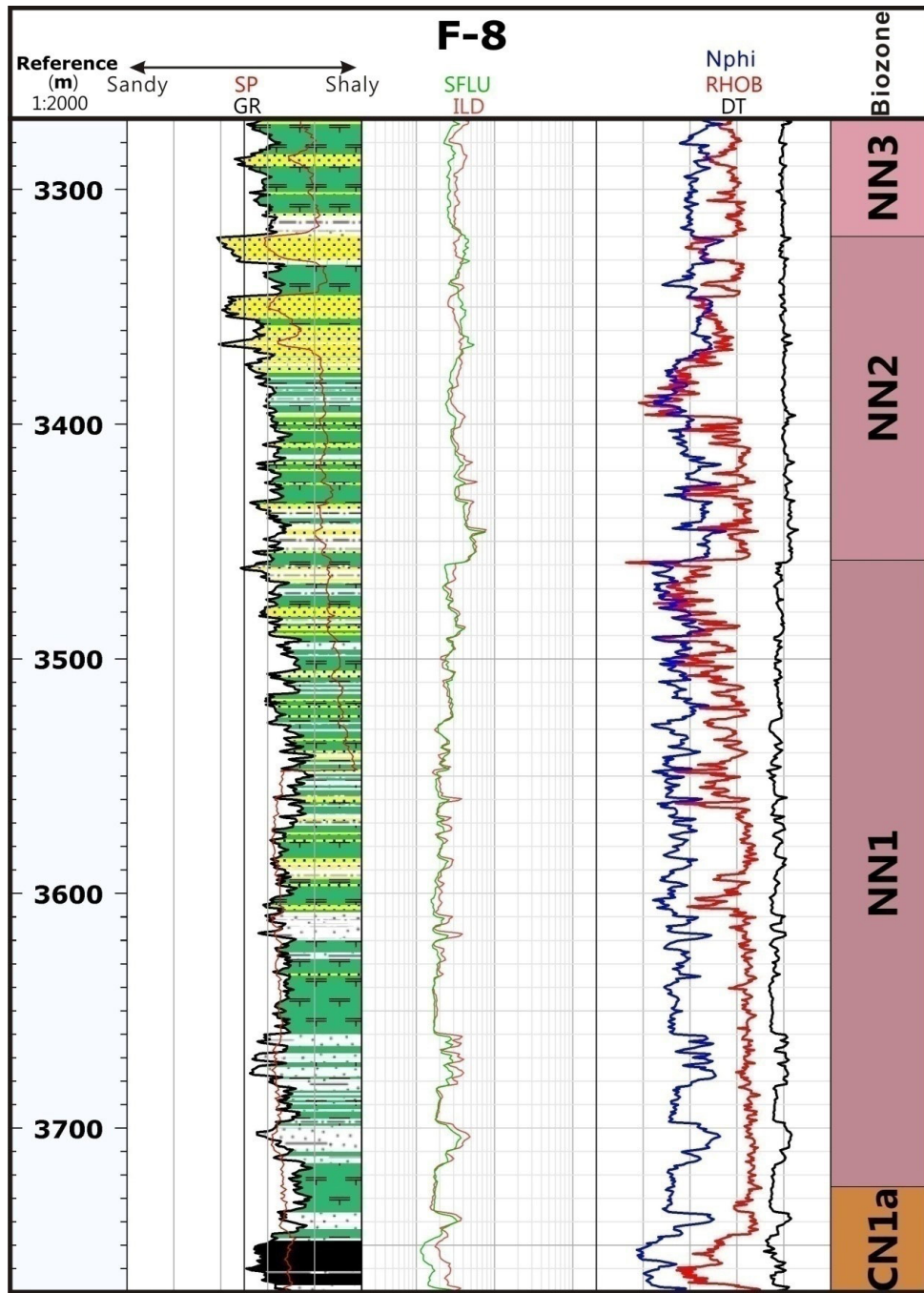


Fig. 4. The composite well log. Showing the integration of the lithology with GR log.

ELECTROFACIES AND DEPOSITIONAL ENVIRONMENT ANALYSIS

Well logs are commonly used for subdividing subsurface strata into different electrofacies with similar patterns. Electrofacies was developed in the last decades and used for sedimentological studies of hydrocarbon reservoirs (Serra, 1989; Posamentier and Allen, 1999). Selley (1978) argued that well-log curves reflect the grain size distribution in sedimentary successions, and thus, the depositional environment. Some classifications are widely used for different log-curve shapes to interpret depositional facies based on log-curve patterns (Serra, 1989; Rider, 1990; Wagoner et al., 1990; Boggs, 1995; Emery and Myers, 1996). GR patterns are the widely used log curves for analysis of subsurface depositional environment (Rider, 1990; Cant, 1992). Cant (1992) divided GR curve shapes into five patterns that reflect different depositional environments, and used SP logs as well. The GR patterns include cylindrical, funnel shape, bell shape, symmetrical, and irregular shapes (Cant, 1992) (Fig 5).

We integrate lithology with Gamma, RHOB, DT, and Resistivity log trends to identify various electrofacies, and conduct a classification of depositional environments (Figure 5 and Figure 6). Table 2 shows the summaries and descriptions for log-curve patterns, electrofacies, and depositional environments. The depositional environments spread from deep to shallow according to the water depth. In this study, we classify the depositional environments into Slope, Turbidite, Outer Offshore, Inner Offshore, Shoreface, Outer Coast, Inner Coast, and Non-Marine (Figure 7). The characteristics of each depositional environment are detailed below.

- (1) Slope: Located in an area with quiet flow regime, mainly suspension mudstone, with ten to tens of meters thick, and is far away from the source of sediment supply, and the sediment often contained nanofossils and planktonic organisms. The high GR and density value indicate high shale content, and GR pattern shows irregular shape with high frequency of change (Fig. 5).
- (2) Turbidite: Slope deposits are often intercalated with turbidite thin beds. It is

characterized by silty mud to fine sand abundant with fossils or fragments. The high GR and density value indicate high shale content, and the GR pattern shows irregular shape with high frequency of change, similar to slope (Fig. 5).

Table 2. Summary of log trends, rock description, electrofacies, and depositional environments.

GR trends	Rhob/DT/Resistivity trends	Rock description(cutting or core)	Electrofacies	Sedimentary Environment Code
High GR API Irregular shape	High density Irregular shape	Massive mud and silty mud	Slope	(1)Slope
		Muddy sand with fine sand interbeds Abundant fossil breccia	Turbidite	(2)Turbidite
GR API decrease upward Funnel shape	High density Irregular shape	Massive mudstone grad to muddy sand	Outer Offshore	(3)Outer Offshore
		Shale or muddy sand grad to vfs-fs Coarsening upward	Inner Offshore	(4)Inner Offshore
Low GR API Cylindrical shape	Low density Cylindrical shape	Massive sandstone	Shoreface	(5)Shoreface
Low GR API Symmetrical shape	High density Symmetrical shape	Massive sandstone with limestone interbeds Calcareous and Carbonaceous	Barrier island	(6)Outer Coast
High GR API Irregular shape	Density drop down Serrated/ DT drop down Cylindrical shape	Massive mud with silty mud interbeds Carbonaceous	Lagoon	
High GR API Irregular shape	High density Density decrease upward Irregular shape	Alternations of sand and shale Sand/shale ratio high	Sand Flat	(7)Inner Coast
	Low density Density decrease upward Irregular shape	Alternations of muddy sand and shale Sand/shale ratio low Shale grad to muddy sand	Mud Flat	
GR API increase upward Bell shape	High density Irregular shape	Massive sandstone with mud-fs interbeds Silty and carbonaceous Lack of fossils	Fluvial	(8)Non Marine
Low GR API Cylindrical shape	Low density Cylindrical shape/ Low resistivity Cylindrical shape	Alternations of shale and silty shale Intercalated coal seam Carbonaceous	Marsh	

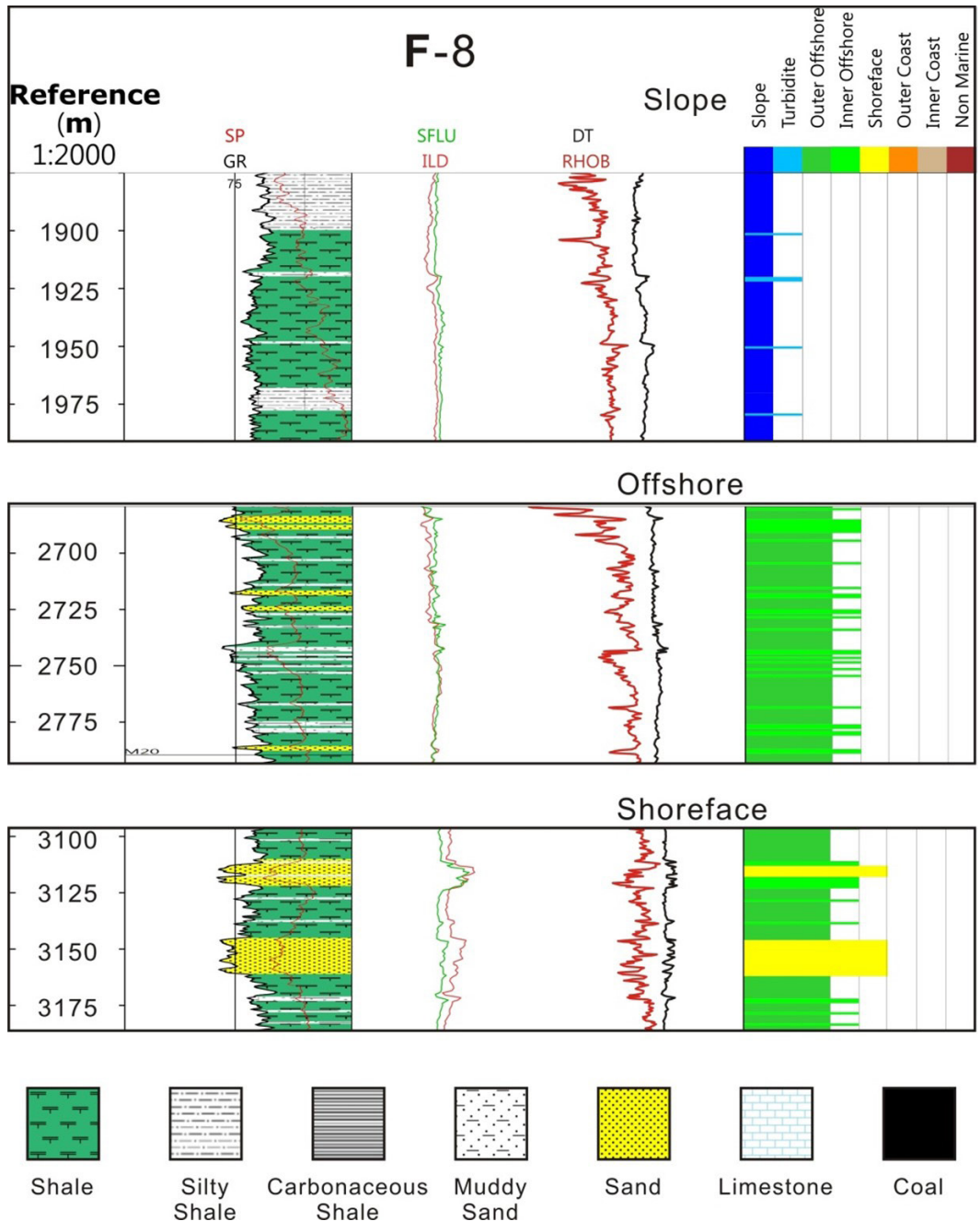


Fig. 5. The interpretation of electrofacies for the depositional environment (shallow marine). Integrating lithology with log trends to define depositional environment.

- (3) Outer Offshore: Deposited below the storm wave base, dominated by suspension deposits. The lithology gradually changes from a massive mudstone to silty mud. The mudstone is usually more than a few meters thick, intercalated coarser sand beds of storm action deposits. Alternations of muddy sand and silty shale are thin-beds between a few centimeters to 1 meter (Dott and Bourgeois, 1982; Reading, 1996; Walker et al., 1983; Walker, 1984). The GR values decrease upward, indicating the shale content decreasing trend, showing a funnel shape (Fig. 5).
- (4) Inner Offshore: Deposited between the fair weather wave base and the storm wave base, it was mainly the accumulation of suspended sediment during fair weather, the coarse sand deposit accumulated during storm weather, and the sediments close to the fair weather wave base were more affected by storms. The beds thickness were usually more than tens of meters, lithology are mainly massive mud and gradually change upward into interbedded sand and mud or muddy sand. The sediment show a coarsening upward pattern by grain size, lithology gradually change from massive mud to sand, and the sand-shale ratio increase upward. Until to the top of inner offshore deposit, the interbedded sand and mud change to massive calcareous sandstone (Dott and Bourgeois, 1982; Reading, 1996; Walker, 1984; Walker et al., 1983). The GR values decrease upward indicating a gradual increase trend of the sand-shale ratio, showing a funnel shape (Fig. 5).
- (5) Shoreface: Deposited above fair weather wave base and below low tide, the sediments were washed by steady and high-energy wave current. The bed thickness is usually more than tens of meters. The lithology is dominated by massive sandstones with carbonaceous matter (Walker and Plint, 1992). The massive sandstone lack of shale contents makes the GR value is distinctly low. The GR pattern shows a cylindrical shape with sharp upper and lower boundaries (Fig. 5).

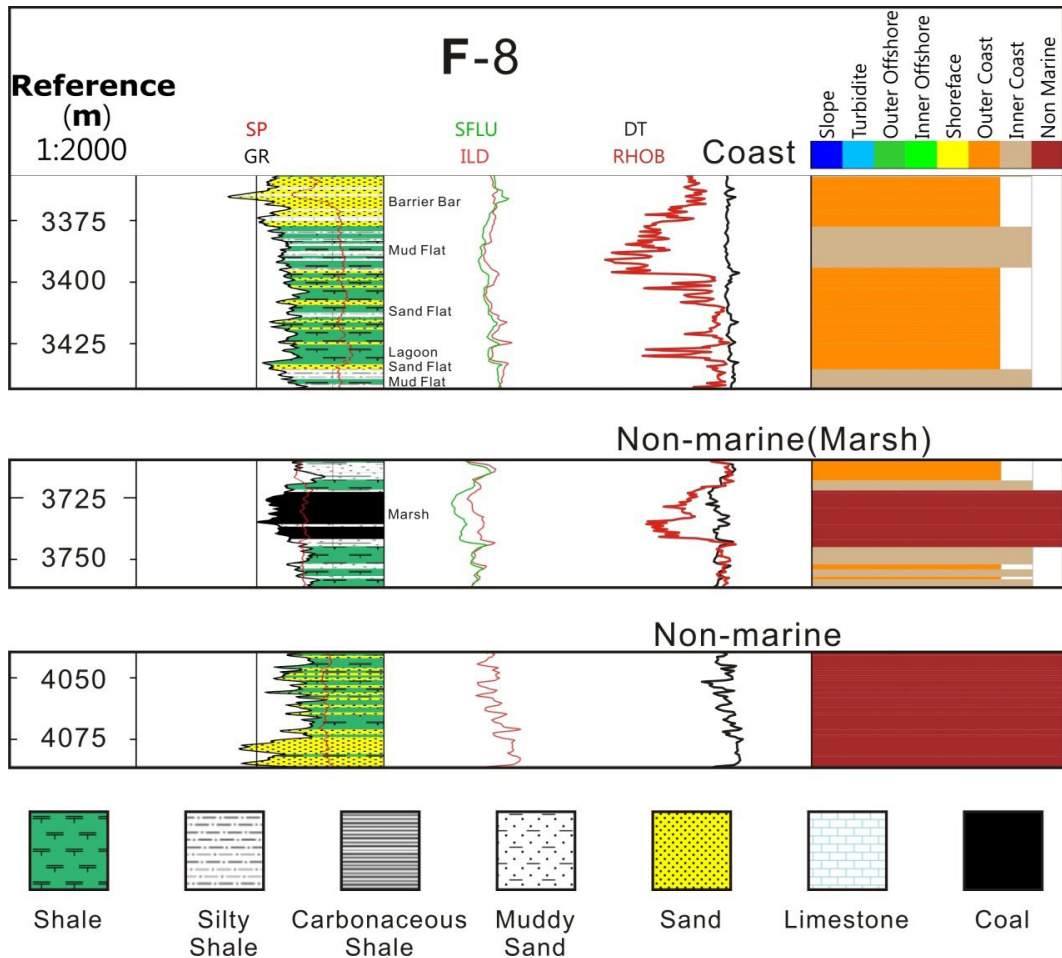


Fig. 6. The interpretation of electrofacies for the depositional environment (coast and non-marine). Integrating lithology with log trends to define depositional environment.

(6) Outer Coast-

Barrier: Affected by the high-energy wave current. The deposits are well sorted with grain size from fine to medium. The thickness of barrier island deposit is several meters to tens of meters, containing calcareous sand, carbonaceous sand and muddy sand (Smd). The well sorting sandstone without matrix contents makes the GR value is distinctly low. The GR value of the muddy sand slightly increase and make the GR pattern show the symmetrical shape (Fig. 6).

Lagoon: Because barrier islands block most wave energy, the coastal areas inside the barrier islands were mainly affected by tidal current. The lagoon was slightly affected by tidal current due to deep water depth where there mainly is the suspended fine grained sediments in quiet flow regime. The thin-laminated mud gradually changed upward to massive mudstone, sometimes intercalated with muddy sand or carbonaceous mud (Dalrymple et al., 1992). The high GR value and irregular GR pattern indicate high shale content, but the soft lagoon sediment and intense bioturbation make the density drop down significantly, showing irregular density curve. Due to the acoustic impedance of the lagoon sediments was relative low, the DT pattern shows a cylindrical shape (Fig. 6).

Sand Flat: Tidal flat belonged to intertidal zone which was between low tide and high tide. Tidal flat was the tidal dominated depositional environment, with alternations of sand and shale formed by bidirectional tidal currents, and the shale content gradually increased from the low tide to the high tide. Intense bioturbation and carbon matters were often observed in tidal flat deposits. Sand flat was the seaward part of tidal flat with lower shale content, and mud flat was the landward part of tidal flat with higher shale content. As the low GR value sand interbedded with high GR value mud, the overall GR value increase, and the GR pattern is irregular serrated shape. The density value is affected by the higher sand-shale ratio of sand flat. The density value of sand flat is obviously higher than that of mud flat, and the Rhob curve shows the irregular shape (Fig. 6)

(7) Inner Coast-Mud Flat: Mud flat was the landward part of tidal flat with higher shale content, with alternations of sand and shale formed by bidirectional tidal currents. Intense bioturbation and carbon matters were often observed in mud flat deposits. The GR pattern of mud flat and sand flat is similar to each, showing irregular shape. The density value is affected by the lower sand-shale ratio of mud flat, the density value of mud flat is obviously lower than that of sand flat, and the Rhob curve shows the irregular shape (Fig. 6).

(8) Non Marine-

Fluvial: Fluvial deposits were commonly fining upward gradually, indicating the process of a river channel changing into floodplain. The lithology was mainly poor to medium sorting sand. Then the sand gradually changed upward into mud. The fluvial sediments were lack of marine fossils, but with high carbon matters content. The GR value gradually increases upwards, and the GR pattern shows the bell shape with distinct base. The density value decreases slightly upwards as the weathered mud content increases, showing an irregular shape (Fig. 6).

Marsh: Marsh environment belonging to quiet flow regime, carbonaceous mud or coal seams were often observed. Density, resistance and the acoustic impedance significantly reduced due to containing loose coal seams. The well-log patterns show the cylindrical shape with distinct upper and lower boundaries (Fig. 6).

SEQUENCE STRATIGRAPHY ANALYSIS

We use the evolution of sedimentary facies to define the transgression and regression system tracts of well F-8. Based on that, the sequence boundary is to be identified (Fig. 7). The trend of sedimentary facies is consistent with the geological framework of Lin (2021). Thus, this study will follow the sequence framework of Lin (2021) to divide Oligocene-Miocene strata into 15 sequences including TO0, TO2, TM0, M2, M4, M6, M8, M10, M12, M14, M16+18, M20, M22, M24 and M26 from bottom to top (Fig. 8).

According to the sequence stratigraphy framework established by Lin (2021), the 15 sequences from the Oligocene to the late Miocene can be divided into four sequence sets: A, B, C, and D. The sequence set A corresponds to the TO0, TO2 and TM0 sequences of the upper Oligocene. The sequence set B corresponds to the M2, M4, M6, M8, M10, M12 and M14 sequences of the lower Miocene. The sequence set C corresponds to the M18 and M20 sequence of the middle Miocene. The sequence set D corresponds to the M22, M24 and M26 sequences of the Upper Miocene. The major horizons for regional correlation are Breakup Unconformity (BU), H-O horizon (Heterolepa-Orbitoid), and Basal Foreland

Unconformity (BFU). The Breakup Unconformity separated the Mesozoic basement from the overlying strata and was the base of the sequence set A. H-O horizon, a fossil condensed section at the top of the sequence set B, indicates a slowly accumulating environment and is an ideal indicator of the maximum flooding surface. Basal Foreland Unconformity at the top of sequence set D separated the Miocene strata from the Pliocene strata.

There are few studies about the Pliocene sequence in the Tainan Basin. Based on the electrofacies and depositional environment analysis results of Well F-8, this study divides the Pliocene strata into sequence P1 and P2. To sum up, this study divides Paleogene-Neogene strata of Well F-8 into a total of 17 sequences based on electrofacies analysis results, as shown in Fig. 9.

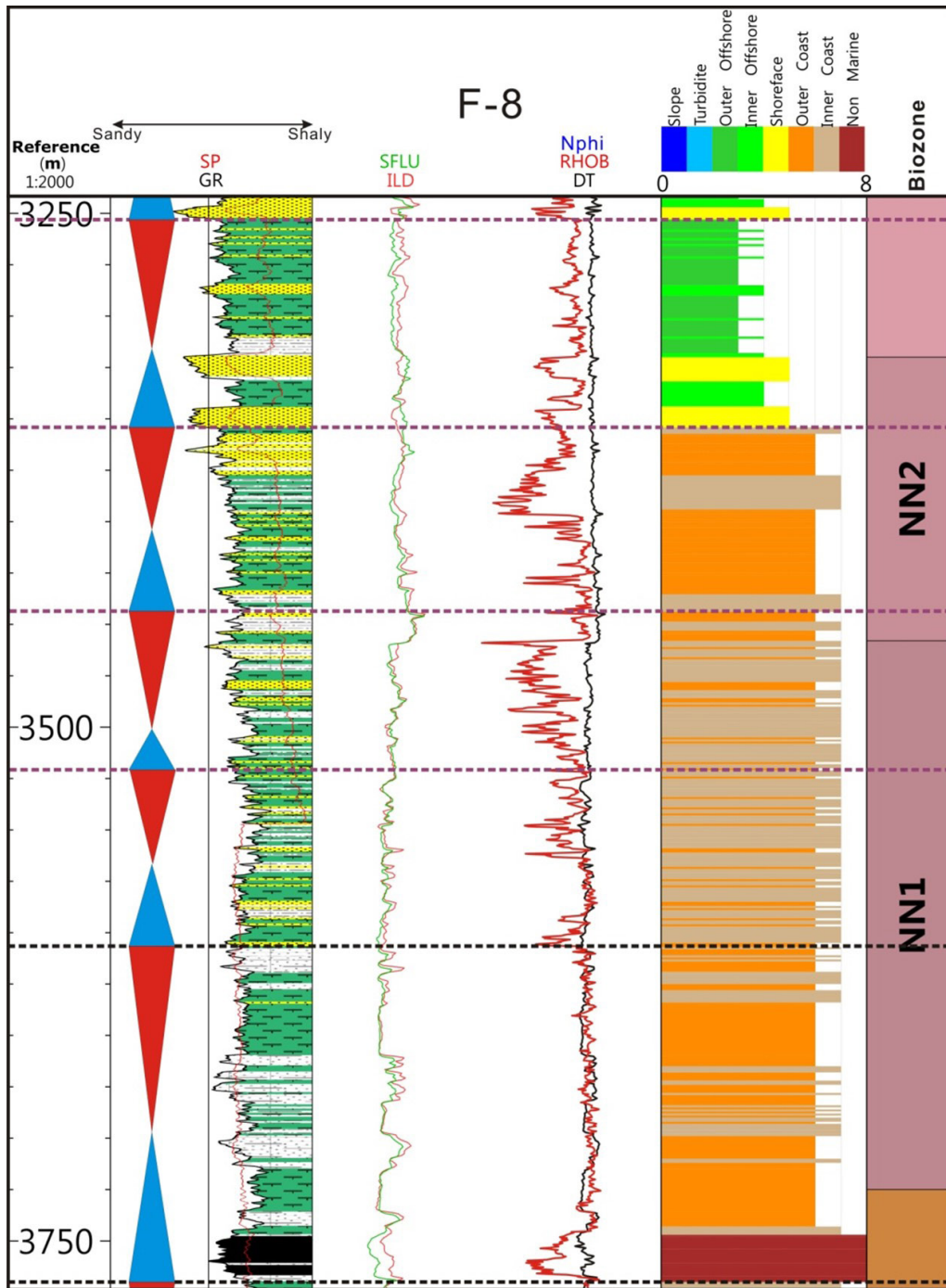


Fig. 7. Identification of sequence boundaries. This example shows the sequence boundaries are defined by transgressive system tract (blue triangle) and regressive system tract (red triangle).

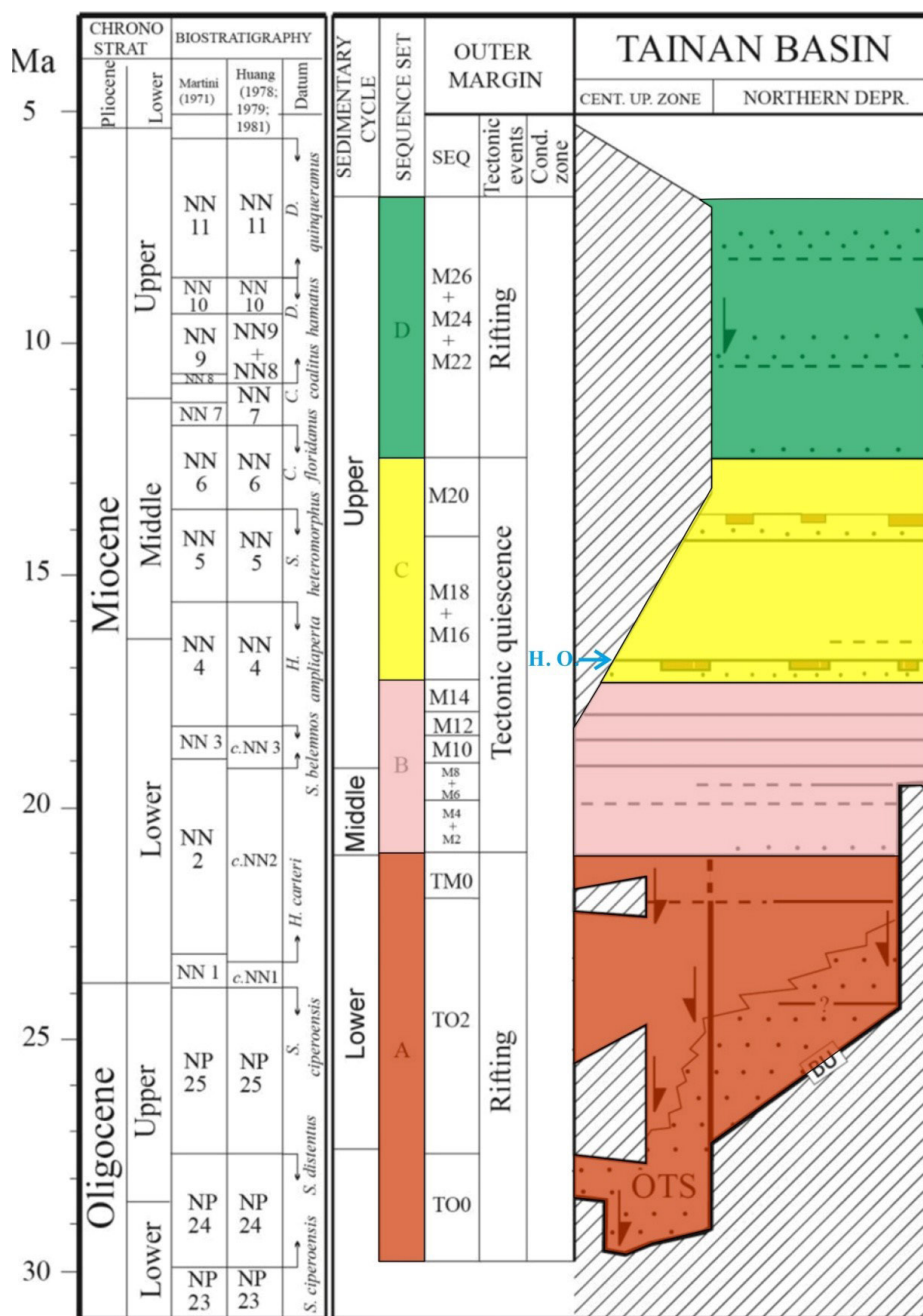


Fig. 8. The chronostratigraphy of the Oligocene-Miocene sequence sets in the Tainan basin (After Lin et al., 2021). Names for defined sequences are shown in the middle column. Dots indicate sandstones and areas with oblique lines indicate hiatus. Thick and short horizontal lines indicate formation boundaries. H.O.: Heterolepa-Orbitoid. OTS: Oligocene Transgressive Sandstone.

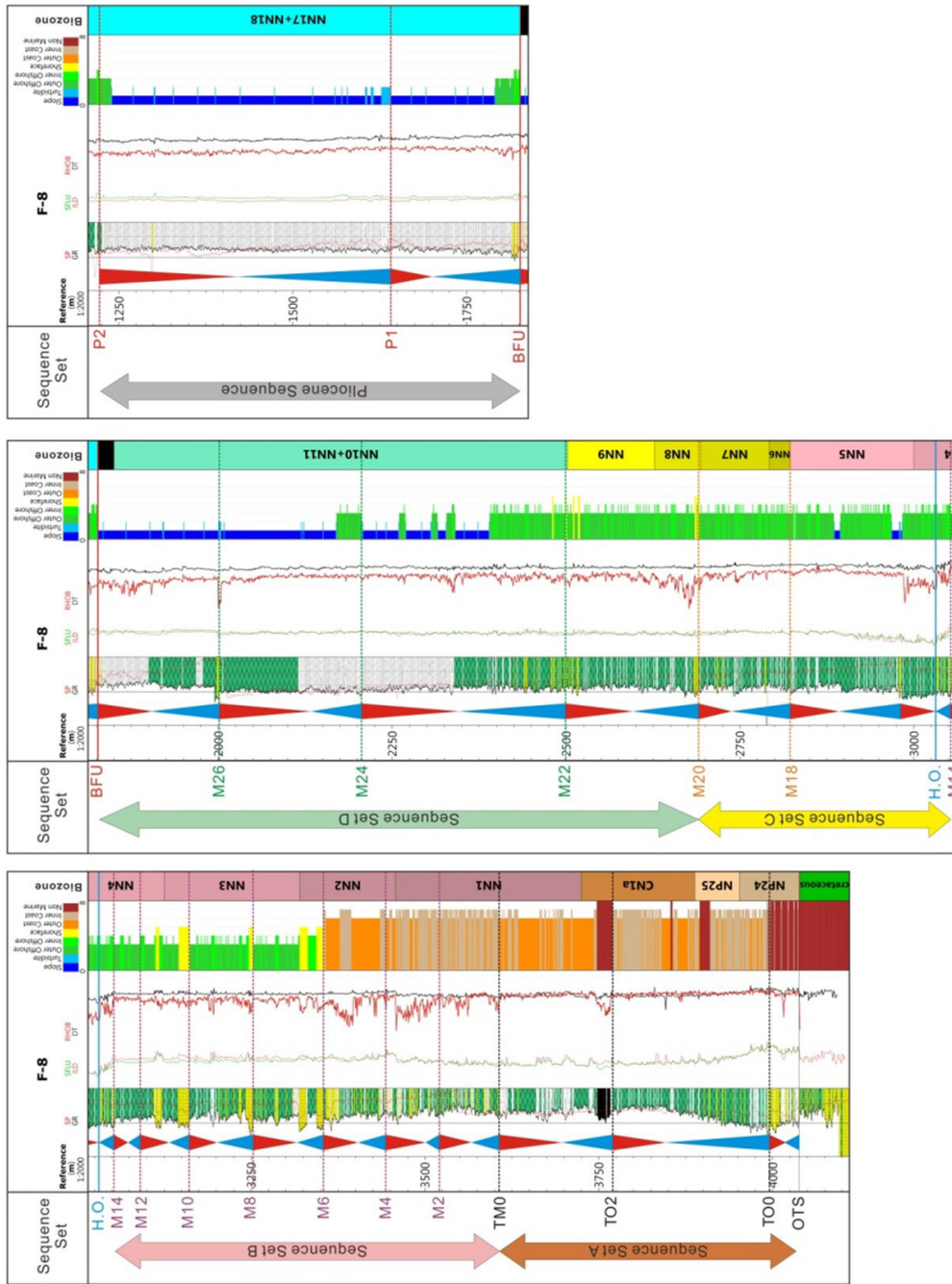


Fig. 9. Sequence stratigraphy analysis results of Well F-8.

BASIN STRUCTURE AND STRATIGRAPHIC FRAMEWORK

The strata of the F-8 well are without hiatus from the late Oligocene to late Miocene based on the nannofossil analysis result. To have a relatively complete chronostratigraphic and depositional environment analysis, the F-8 well is used as a reference well for the sequence stratigraphic correlation profile in the Tainan Basin. This study builds the sequence correlation profile by connecting the wells from north to south, including C-1, P-1, Y-1, J-1, FF-1, F-8, F-6, F-10, and M-1 wells (Fig. 2). According to the definition of Lin (2021), the H-O horizon is the maximum flooding surface in the late Early Miocene suitable as a reference horizon. The methods of creating the sequence stratigraphic correlation profile are as follows: (1) Take the H-O horizon as the reference top of the sequence set A and B to explain the geological framework of the early Miocene strata; (2) Take the BFU horizon as the reference top of the sequence set C and D to explain the influence of rift activities on the morphology of the basin of the late Miocene; (3) Build the Pliocene sequence correlation profile to discuss the tectonic characteristics of the foreland basin formed by orogenic loading. The results of sequence stratigraphy correlation are described below.

1. Sequence set A and sequence set B: TO0-M14, refer to Fig. 10.

In Fig. 10, the Mesozoic basement top is marked by the thick black solid line; the H-O horizon as the reference top of the sequence set A and sequence set B is marked by the blue solid line; the tops of each sequence of the sequence set A, including the TO0, TO2, and TM0 sequences, are marked by the black dashed line; the tops of each sequence of the sequence set B, including from the M2 to the M14 sequence, are marked by the purple dashed lines.

The geological framework of sequence set A shows that the extensional structures dominated the evolution of the basin morphology during the initial rift stage. The TO0 sequence was mostly deposited in the area south of the F-6 well, and some minor normal faults are observed on both sides of well F-6. Due to the continuous rifting activities, the range of extensional structures and grabens increased, and the area covered by the TO2 sequence expanded to the southern P-1 well. The rapidly increased accommodation made the non-marine depositional

environment become the outer coast depositional environment, causing a fining-upward sediment particle pattern. After the deposition of the TM0 sequence, the subsidence rate was gradually slow down. At this time, the sediment deposition rate and the accommodation increasing rate were about the same, leading to aggradation-pattern parasequences.

The TM0 sequence belonged to the lowstand system tract, non-marine sediment deposited on the base, and overlaid by the inner to outer coast sediments with aggradation pattern.

In sequence set B in the area south of Well P-1, the M2, M4, and M6 sequences belong to subsidence basins. During this period, the sediment deposition rate and the accommodation increase rate were about the same, resulting in the inner to the outer coast depositional environment. The accommodation increase rate of the M8 sequence began to exceed the sediment deposition rate, causing the relative sea level to rise gradually. Therefore, the depositional environment changed from the outer coast to the offshore environment. After well correlation, we believe that the M8 and M10 sequences were deposited not only in the southern area but also in the northern P-1 and C-1 well. The depositional environments of the M10 to M14 sequences were mainly offshore. Besides, the M8-M14 sequences of the southernmost M-1 well were all missing, which is different from the neighboring areas. It was inferred that there should be a fault between the M-1 well and the northern area as a tectonic boundary. The south of the fault is a relatively topographic high without sedimentation, the erosion surface or strata hiatus happened there. In summary, when the M8 sequence was deposited, the rifting had stopped with no more faulting. Thus, the relative sea-level gradually rose, and the depositional environment changed from the outer coast to the offshore.

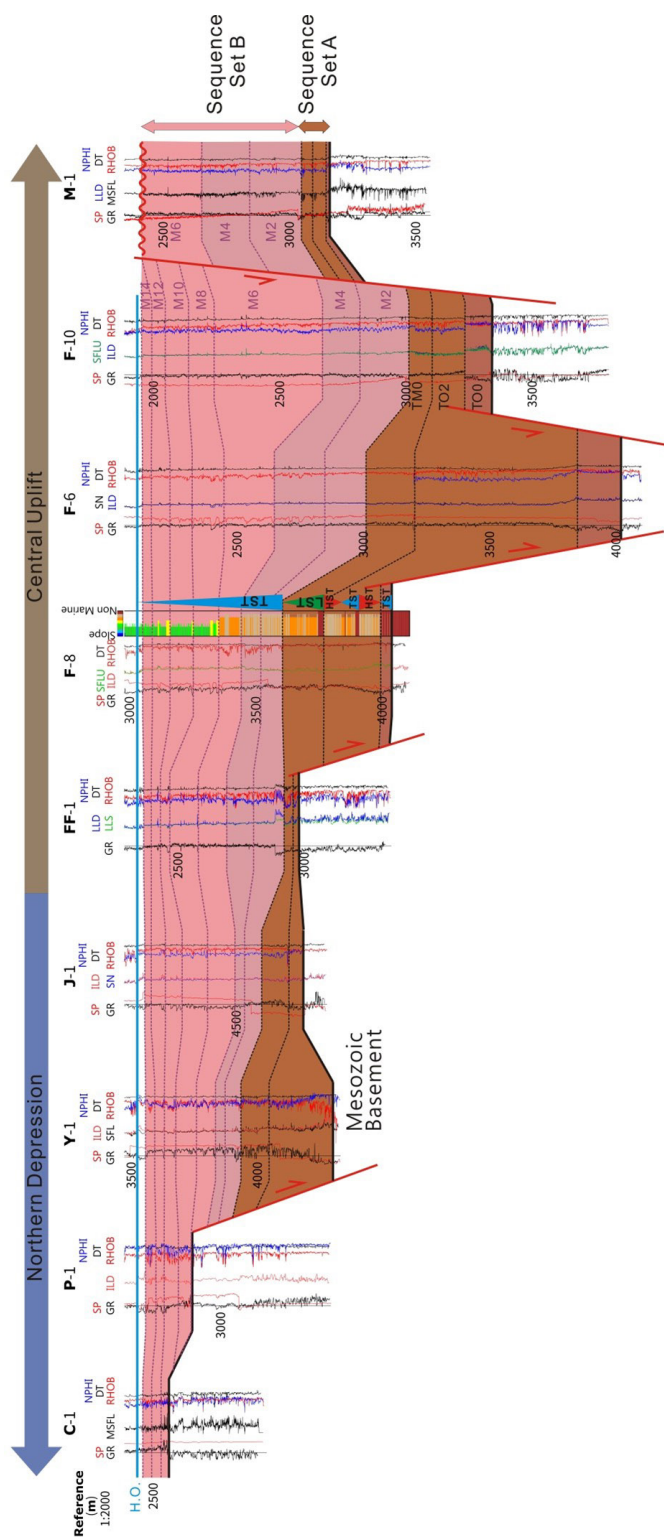


Fig. 10. Geological framework of the sequence set A and sequence set B. The sequence set A, containing TO0, TO2, and TM0 sequences, was deposited during the late Oligocene to early Miocene; the sequence set B, containing sequences from M2 to M14, was deposited during the early Miocene. Red solid lines indicate faults, and the red wavy line indicates unconformity.

2. Sequence set C and sequence set D: M18-M26, refer to Fig. 11.

The thick red solid line indicates the Basal Foreland Unconformity (BFU). The blue solid line indicates the H-O horizon. The orange dashed lines indicate the top of each sequence of the sequence set C, including the M16+18 and M20 sequences. The green dashed lines indicate the top of each sequence of sequence set D, including the M22 to M26 sequences.

Sequence set C, containing M16+18 and M20 sequences, was deposited during the highstand period in the middle Miocene. During the deposition of the M16+18 sequences, there were multiple transgressive events, causing the depositional environment to change from offshore to slope. The H-O horizon was the most obvious transgressive event shown on well log curve, so the H-O horizon was taken as the regional reference horizon of the Tainan Basin. During the deposition of the M20 sequence, the sediment deposition rate began to exceed the accommodation increasing rate, resulting in an unconformity in the local topographic high areas at the south of the F-6 and FF-1 wells, and the erosion generally occurred at the top of the sequence.

The sequence set D, containing M22, M24, and M26 sequences, was deposited during the late Miocene. The topographic high area, at the south of the F-6 well, was the Central Uplift Zone with the sequence set D hiatus. It is inferred that there should be a fault between the F-6 well and F-8 well as a tectonic boundary of the northern subsidence area and the Central Uplift Zone.

In the northern subsidence area, the M22 sequence deposited in shoreface and offshore was widespread in most wells except for the FF-1 well. While the M24 and M26 sequences were deposited, the strata in the northern subsidence area were much thicker, and the depositional environment changed from offshore to slope, indicating the rapid increase in accommodation. However, the thickness of the M24 and M26 sequences of the FF-1 well was relatively thinner than other wells in the northern subsidence area, suggesting that the FF-1 well is located on a relative topographic high area. We think that the relatively topographic high area separates the F-8 well on the south and the C-1, P-1, Y-1, and J-1 wells on the north. According to previous studies, the northern subsidence area where the C-1,

P-1, Y-1, and J-1 wells are located belong to the Northern Depression (Lee et al., 1995), while the area of the F-8 well was not defined yet.

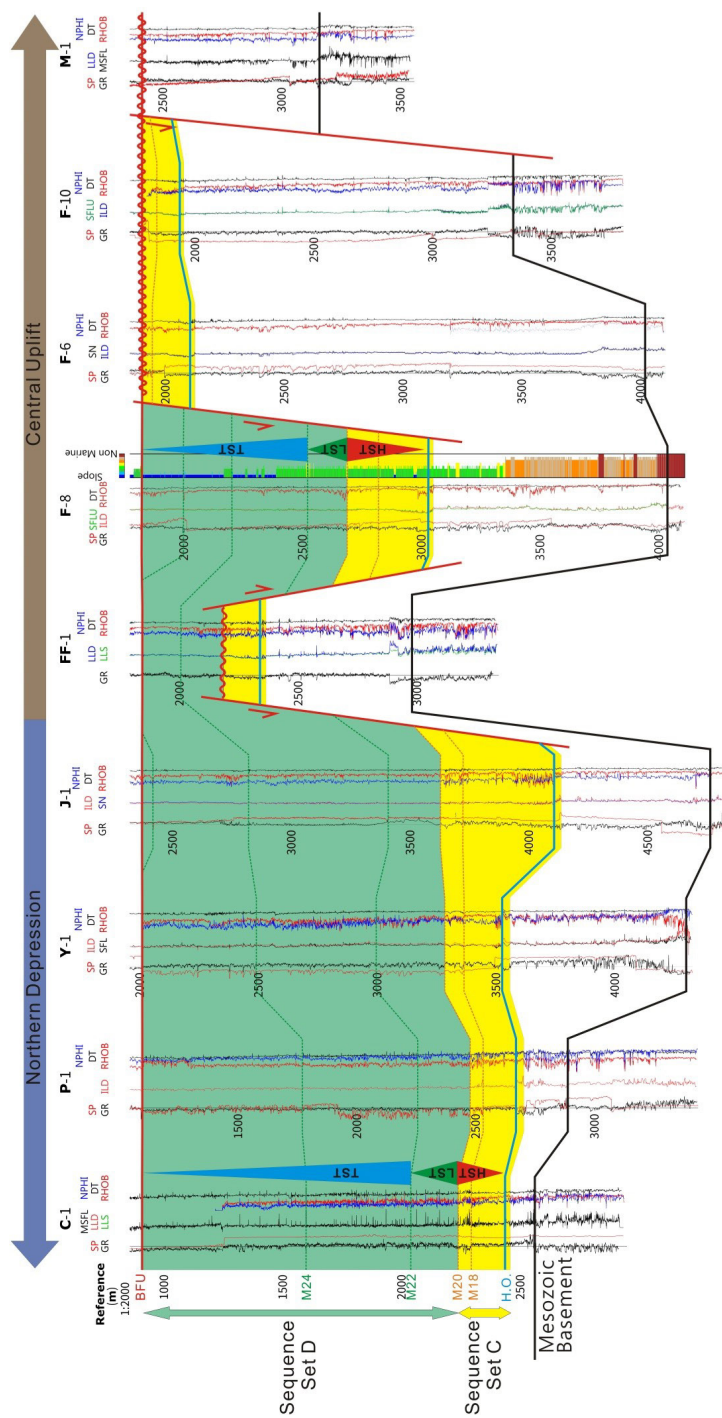


Fig. 11. Geological framework of the sequence set C and sequence set D. The sequence set C, containing M16+18 and M20 sequences, was deposited during the early Miocene to middle Miocene; the sequence set D, containing sequences from M22 to M26, was deposited during the middle Miocene to late Miocene. Red solid lines indicate faults, and the red wavy lines indicate unconformities.

3. Pliocene sequence: P1 and P2, refer to Fig. 12.

In the Pliocene stratigraphic correlation profile, the Pliocene strata can be divided into the P1 and P2 sequences. The P1 sequence of the P-1 well was the thickest in the northern subsidence area, but it is missing in the southernmost M-1 well. The depositional environment of the P1 sequence was still the slope environment with deep water depth.

Table 3. Summary of the sequence analysis results of 9 wells used in this study. The numbers indicate the depth of each sequence top.

	C-1	P-1	Y-1	J-1	FF-1	F-8	F-6	F-10	M-1	
P2	524	378	910	1333	1237	1522	1170	1165	1497	
P1	651	576	1660	2149	1706	1640	1713	1697	S.U.	
BFU	910	1097	2009	2375	1845	1827	1903	1779	2420	
M26	S.U.	S.U.	S.U.	2421	S.U.	2004	S.U.	S.U.	S.U.	
M24	1600	1770	2490	2824	2008	2206				
M22	2040	2256	2975	3185	S.U.	2249				
M20	2241	2478	3283	3622		2692				
M18	2296	2533	3364	3723	2185	2823	1945	1840		
H.O.	2440	2670	3526	4110	2340	3031	2105	1930		
M14	2457	2708	3553	4139	2363	3058	2134	1955		
M12	2498	2743	3587	4170	2395	3086	2175	1992		
M10	2533	2778	3633	4221	2434	3162	2241	2047		
M8	2563	2833	3679	4287	2469	3254	2314	2140		
M6	S.U.	2885	3783	4332	2580	3355	2445	2240		
M4		S.U.	3834	4495	2692	3440	2637	2670		2654
M2			3873	4535	2870	3520	2748	2820		2843
TM0			3937	4603	2923	3605	3014	3013	3047	
TO2			4046	4710	2962	3770	3215	3103	3094	
TO0			S.U.	S.U.	S.U.	3995	3847	3233	3146	
OTS			2583	2889	4300	4767	2980	4038	4024	3340
Remark	S.U. indicates Subaerial Unconformity. OTS indicates Oligocene Transgressive Sandstone. The black numbers are from Lin (2021) sequence analysis results. The red numbers and text are sequence analysis results in this study.									

The thickness of the P2 sequence in the Y-1, J-1, FF-1, F-8, F-6, and F-10 well is significantly thicker than that of the P1 sequence, and the deposition of the P2 sequence started on the southernmost M-1 well. The rapid increase in accommodation, caused by the regional depression activity, resulted in the thickness difference of the P1 and P2 sequences. However, the thickness of the P2 sequence in C-1 and P-1 wells was thinner than that of the P1 sequence. According to the difference in the amount of subsidence between the north and south, we infer that there is a fault between the P-1 well and Y-1 well as a tectonic boundary.

DISCUSSION

We create a chronostratigraphic chart that integrated the sequence stratigraphy analysis result from Lin (2021) with the eustatic curve, and depositional environment analysis, as shown in Fig. 13. This study talks about the tectonic behavior and characteristics during the post-breakup stage and the foreland basin stage based on the geological framework of the sequences from TO0 to P2 in the Tainan Basin.

The sequence set A, containing the TO0, TO2, and M20 sequences, was deposited during the late Oligocene to early Miocene, which corresponds to the TB1.1, TB1.2, TB1.3, and TB1.5 cycles of the eustatic sea-level curve. This period belongs to the early post-breakup stage of Lin (2003). Although the eustatic sea level was highstand during this period, the accommodation increased in the grabens due to activities of normal faults. The TO0 sequence was only observed in the F-6 well, which showed that the distribution of the initial grabens was quite restricted with the shallow-water depositional environment. While the TO2 sequence was deposited, the area south of well F-8 began to subside, and the grabens area began to expand. While the TM0 sequence was deposited, the southern area of the P-1 well became the subsided basin. After that, the tectonic activities in the Tainan Basin gradually slowed down, and the area of grabens no longer expanded. In this study, the tectonic behavior during this period in the Tainan Basins was consistent with the initial subsidence tectonic activity (32-22 Ma) of Lee (1993) or the early post-breakup tectonic activity (30Ma~21Ma) of Lin (2003).

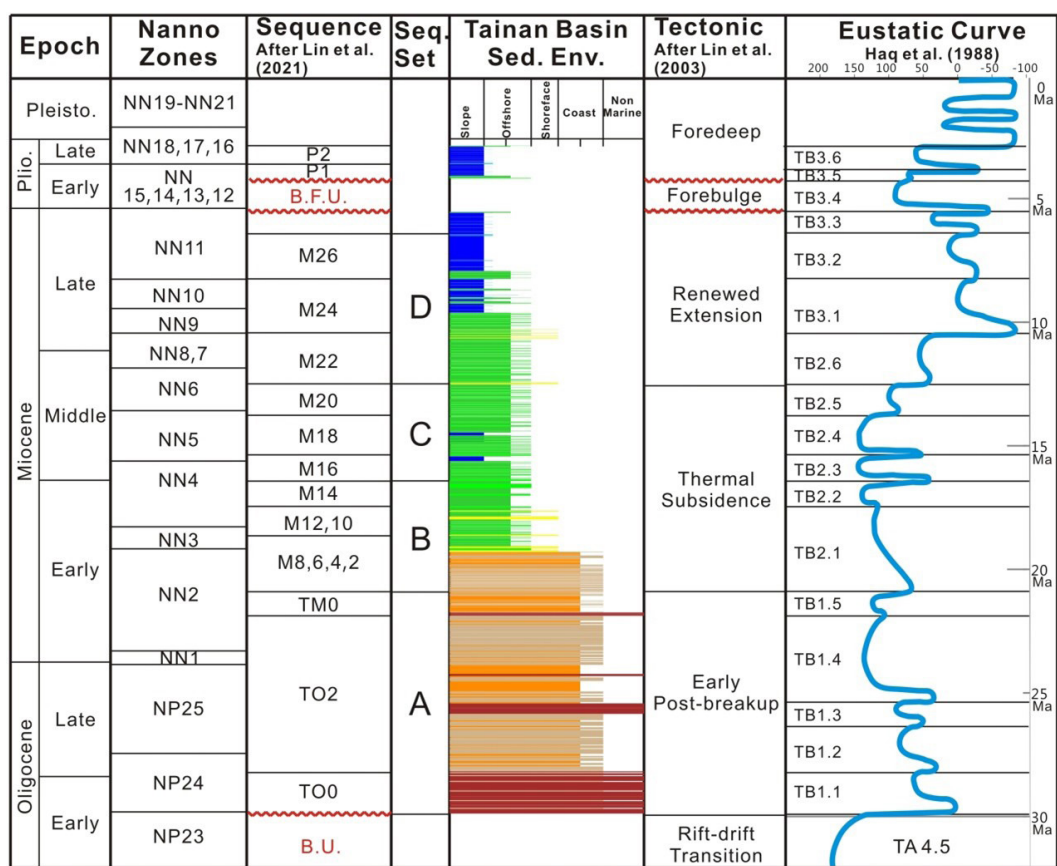


Fig. 13. Chronostratigraphic chart integrated the sequence stratigraphy and eustatic curve with depositional environment analysis results of this study (After Lin et al., 2021). The Cenozoic time scale is based on the result of Berggren (1995). The nanno zones are based on the result of Huang T.C. (1982). The age of the sequences from TO0 to M26 is based on the result of Lin (2021) BU: Breakup unconformity, BFU: Basal Foreland Unconformity.

The sequence set B and set C, containing the M2 to M20 sequences, were deposited during the early and middle Miocene, which corresponds to TB2.1 to TB2.5 cycles of the eustatic sea-level curve. This period was quiescent for the tectonic activity of Lin (2003), so the increasing accommodation was caused by thermal subsidence. The depositional environments were gradually deeper during the highstand period. As a result, the increasing rate of the accommodation was roughly equal to the sediment depositional rate, so the depositional environment remained offshore.

However, in the southernmost M-1 well, there is a hiatus appeared in the M8 sequence. Based on the missing strata from the M8 to M14 sequences in the M-1 well, we infer there should be a fault between the well M-1 and the northern area as a tectonic boundary. This fault might have been formed after the deposition of the M6 sequence, and a topographic high area formed on the hanging wall side.

Due to the falling of the eustatic sea level, there are several unconformities in the M20 sequence in the local topographic high areas where the F-6, F-10, M-1, and FF-1 wells are located. Those erosion surfaces are generally at the top of the sequence.

The sequence set D, containing the M22, M24, and M26 sequences, was deposited during the middle Miocene to the late Miocene, which corresponds to the TB2.6, TB3.1, TB3.2, and TB3.3 cycles of the eustatic sea-level curve. Due to the lowstand period, the sequence set D was missing in the F-6, F-10, and M-1 well. It is thought that there is a topographic high area with sequence set D hiatus. According to previous studies, the topographic high area, where the F-6, F-10, and M-1 wells were located, belonged to the Central Uplift Zone (Lee et al., 1995). However, the sequences set D of the F-8, J-1, Y-1, P-1, and C-1 wells were thicker, and the depositional environment changed from offshore to the slope. It is shown that the accommodation increased rapidly during this period in the area, but the result was inconsistent with the trend of the eustatic sea-level curve. We infer that the increase of accommodation was dominated by renewed extension activities of Lin (2003). The subsidence area formed by the renewed extension activities was called the Northern Depression (Lin et al., 2003; 2021). Because the tectonic behavior of the Northern Depression was different from that of the Central Uplift Zone, we infer that there should be a fault between the F-6 and F-8 wells as a tectonic boundary.

The Pliocene strata include the P1 and P2 sequences. According to the nannofossil zones of the 9 wells used in this study, the NN12-NN14 strata were generally missing. It corresponds to the TB3.5 and TB3.6 cycles of the eustatic sea-level curve. The depositional environment was a slope with deep-water depth.

The stratigraphic hiatus in the early Pleistocene is worth being studied. The

hiatus strata corresponded to the TB3.5 cycle of the eustatic sea-level curve, which belonged to the period when sea level rose to highstand. Obviously, the eustatic sea-level change is not the reason for the missing of the NN12-NN14 strata. It is inferred that due to tectonic uplift, there were several widespread unconformities of the NN12-NN14 strata in the Tainan Basin. It is inferred that the regional tectonic uplift is a forebulge deformation due to the lithosphere bending on the margin of the foreland basin.

The thickness of the Pliocene sequences in the Y-1, J-1, FF-1, F-8, F-6, and F-10 wells was quite thick, which was caused by the development of the foredeep basin. However, the thickness of the P2 sequence in C-1 and P-1 wells was thinner than that of the P1 sequence. It is inferred that the forebulge migrated toward the Penghu Platform and the initial subsidence area gradually became stable. Due to the difference in subsidence rate, it could be seen that a fault had developed between the P-1 and Y-1 wells.

SUMMARY AND CONCLUSION

Traditional subsurface stratigraphic correlations are mostly based on well log curves. The stratigraphic correlations between well logs were widely used for their simplicity and speed. However, there are many uncertainties if we only use well log data for depositional environment analysis or sequence stratigraphic analysis. Therefore, we integrated the lithology analysis results of rock description with electrical log curve to improve the accuracy of lithology interpretation.

We integrate the lithology with the electrical log patterns to define the electrofacies, used for the interpretation of the depositional environment of the subsurface strata. We divided the formation of the F-8 well into 8 depositional environments, which were Slope, Turbidite, Outer Offshore, Inner Offshore, Shoreface, Outer coast, Inner Coast, and Non-Marine.

The electrofacies and the depositional environment analysis of well log data were applied to the sequence stratigraphic analysis. Based on the trend of the sedimentary facies, we can define the transgression and regression system tracts of the F-8 well as the basis for finding the sequence boundaries. We also refer the results to the sequence stratigraphic framework established by Lin et al. (2021), in

which the Oligocene-Pliocene strata of the F-8 wells are divided into 17 sequences as the basis for regional correlation in the Tainan Basin.

Based on the analysis results of the depositional environment, it is found that the accommodation increased rapidly in sequence set D due to the renewed extension activities during the middle Miocene to the late Miocene. While sequence set D was deposited, the Northern Depression began to form. The range of the Northern Depression could extend the south area where the F-8 well is located, rather than being limited to the subsidence area north of the FF-1 well. We infer that there should be a fault between the F-6 and F-8 wells as a tectonic boundary of the Northern Depression and Central Uplift Zone.

The general lack of early Pliocene strata above the Basal Foreland Unconformity (BFU) in the Tainan Basin was inferred to be related to the forebulge deformation due to the lithosphere bending on the margin of the foreland basin. The regional tectonic uplift caused by the forebulge made the general missing of the NN12-NN14 nannofossil strata.

During the Pliocene sequences deposited, the thickness of the Pliocene sequences in the Y-1, J-1, FF-1, F-8, F-6, and F-10 wells was significantly thicker, which was caused by the development of the foredeep basin. The initial subsidence area where the well C-1 and P-1 were located gradually stopped sinking. It could be seen that a fault had developed between the P-1 and Y-1 wells.

REFERENCES

- Berggren, W.A., Kent, D.V., Swisher III, C.C., and Aubry, M.P.**, 1995, A revised Cenozoic geochronology and chronostratigraphy. In: Berggren, W.A., Kent, D.V., Aubry, M.-P., Hardenbol, J. (Eds.), *Geochronology Time Scales and Global Stratigraphic Correlation*, Society of Economic Paleontologists and Mineralogists Special Publication 54, pp. 129-212.
- Boggs, S.**, 1995, *Principles of sedimentology and stratigraphy* (p.784), Toronto: Merrill Publishing Company.
- Cant, D.**, 1992, Subsurface facies analysis, In R. G. Walker (Ed.), *Facies models, response to sea level changes* (pp. 27-45), St. John's: Geological Association of Canada.
- Dalrymple, R.W., Zaitlin, B.A., and Boyd, R.**, 1992, Estuarine facies models: Conceptual Basis and Stratigraphic Implications, *J. Sedim. Petrol.*, 62, 1130-1146.

- Dott, R.H.Jr., and Bourgeois, J.**, 1982, Hummocky stratification: Significance of its variable bedding sequences, *Geol. Soc. Am. Bull.*, 93, 663-680.
- Emery, D., and Myers, K.J.**, 1996, *Sequence stratigraphy* (p. 297). Hoboken: Blackwell Science Limited, <https://doi.org/10.1002/9781444313710>
- Haq, C.R., B.U., Hardenbol, J., and Vail, P.R.**, 1987, Chronology of fluctuating sea levels since the Triassic, *Science*, v. 235, p. 1156-1167.
- Huang, T.C.**, 1982, Tertiary calcareous nannofossil stratigraphy and sedimentation cycles in Taiwan, *Proceedings of the Second ASCOPE Conference and Exhibition*, Manila, Philippines, pp. 837-886.
- Lee, C.I., Oung, J.N., Ke, H.W., Lin, L.H., Chiou, T.Y., and Huang, T.H.**, 1995, Petroleum System of the Tainan Basin, Exploration & Development Research Institute internal report.
- Lin, A.T., and Watts, A.B.**, 2002, Origin of the West Taiwan basin by orogenic loading and flexure of a rifted continental margin, *Journal of Geophysical Research, Solid Earth*, v. 107, no. B9, p. ETG 2-1-ETG 2-19.
- Lin, A.T., Watts, A.B., and Hesselbot, S.P.**, 2003, Cenozoic stratigraphy and subsidence history of the South China Sea margin in the Taiwan region, *Basin Research*, 15, p.453-478.
- Lin, A.T., Yang, C.C., Wang, M.H., and Wu, J.C.**, 2021, Oligocene-Miocene sequence stratigraphy in the northern margin of the South China Sea: An example from Taiwan, *Journal of Asian Earth Sciences*, v.213, pp. 25.
- Posamentier, H.W., and Allen, G.P.**, 1999, *Siliciclastic sequence stratigraphy: concepts and applications* (Vol. 7, p. 210), Tulsa, Oklahoma: SEPM (Society for Sedimentary Geology).
- Reading, H.G., and Levell, B.K.**, 1996, Controls on the sedimentary rock record. In Reading, H.G. (ed), *Depositional environments: Processes, Facies and Stratigraphy*, 3rd Edition. Blackwell Science Ltd., Oxford, 5-36.
- Rider, M.H.**, 1990, Gamma-ray log shape used as a facies indicator: critical analysis of an oversimplified methodology, *Geological Society, London, Special Publications* (pp. 27– 37). <https://doi.org/10.1144/GSL.SP.1990.048.01.04>.
- Selley, R.C.**, 1978, Concepts and methods of subsurface facies analysis, *American Association of Petroleum Geologists ContinEduc Course Notes Ser*: 9–82.
- Serra, O.**, 1989, *Depositional environments from wireline logs*, Schlumberger Educational Services.
- Sun, S.C.**, 1985, The Cenozoic tectonic evolution of offshore Taiwan, *Energy*, v.10, p.421-432.
- Teng, L.S.**, 1987, Stratigraphic records of the late Cenozoic Penglai orogeny of Taiwan, *Acta Gwl. Taiwan.*, no.25, p. 205-224.
- Teng, L.S.**, 1990, Geotectonic evolution of late Cenozoic arc-continent collision in Taiwan, *Tectonophysics*, no.183, 57- 76.

- Teng, L.S., and Lin, A.T.**, 2004, Cenozoic tectonics of the China continental margin: Insights from Taiwan, Aspects of the Tectonic Evolution of China, Geological Society, London, Special Publications, 226, pp. 313-332.
- Van Wagoner, J.C., Mitchum, R.M., Campion, K.M., and Rahmanian, V.D.**, 1990, Siliciclastic sequence stratigraphy in well logs, cores and outcrops, AAPG Methods in Exploration, no. 7, 55 p.
- Walker, R.G., Duke, W.L., and Leckie, D.A.**, 1983, Hummocky stratification: Significance of its variable bedding sequences: Discussion. Geol. Soc. Am. Bull., 94, 1245-1249.
- Walker, R.G.**, 1984, Shelf and shallow marine sands, Facies models, 2nd Edition, Geol. Assoc. Can., Waterloo, Ontario, 1-14.
- Walker, R.G., and Plint, A.G.**, 1992, Wave-and storm-dominated shallow marine systems, Facies Models Response to Sea Level Change, Geol. Assoc. Canada, 219-238.

台南盆地古近紀-新近紀地層之電測相與層序地層 初步研究

蘇清全¹ 涂嘉勝¹ 林殿順² 謝秉融¹

摘要

電測相常用於判釋沉積環境，原理是藉由電測曲線的形貌進行電測相分類，以GR電測曲線的應用最為廣泛。然而若僅依靠電測曲線之形貌判釋沉積環境，其分析結果存在較多不確定性。因此本研究整合井下地質報告中的岩屑描述資料和電測曲線形貌定義電測相，大幅減少沉積環境分析結果之不確定性。

為了解台南盆地沉積環境變化，本研究以F-8井做為電測相與沉積環境分析之標準地層柱。古近紀-新近紀地層之沉積環境可劃分為以下8種沉積環境，分別為斜坡、濁流岩、外遠濱、內遠濱、濱面、外部近岸、內部近岸和陸相。根據沉積環境的變化趨勢，將漸新世-上新世地層劃分為17個層序，作為台南盆地區域對比的依據。

根據本研究構建之層序對比剖面，探討台南盆地漸新世至上新世的地質架構。晚漸新世至早中新世堆積的層序組A，對應於台南盆地後張裂構造期的早期。早中新世至中新世的層序組B和層序組C，沉積當時台南盆地之構造活動較為平靜，沉積空間主要是由熱沉降作用提供。於中中新世至晚中新世堆積的層序組D，沉積當時台南盆地的張裂構造再次活動，使得沉積環境並未隨著全球海水位的下降而變淺，沉積環境反而逐步加深，這個時期形成的張裂盆地稱為北部凹陷。北部凹陷以南的中央隆起帶受全球海水位下降的影響，普遍缺失層序組D，推測F-6井與F-8井之間應存在斷層作為構造邊界。上新世地層普遍缺少NN12-NN14 超微生物帶地層，其對應到的TB3.5海水位循環屬於海水位上升之高水位時期，初步排除海水位變動造成地層缺失的可能性，因此推論地層缺失的現象為前陸盆地之前緣隆起變形所致。直到上新世層序沉積，前淵盆地之發育使得沉積物厚度明顯增厚，但在靠近澎湖地台的地區此現象並不顯著。

關鍵詞：電測相、台南盆地、層序地層分析

¹ 台灣中油股份有限公司探採研究所

² 國立中央大學地球科學系